SKIN-FRICTION DRAG REDUCTION USING THE METHOD OF SPANWISE MEAN VELOCITY GRADIENT

Jens H. M. Fransson
Linné Flow Centre
Department of Mechanics
KTH–Royal Institute of Technology
SE–100 44 Stockholm, Sweden
jensf@kth.se

Robert S. Downs III
Linné Flow Centre
Department of Mechanics
KTH–Royal Institute of Technology
SE–100 44 Stockholm, Sweden
downs@mech.kth.se

Sohrab S. Sattarzadeh
Linné Flow Centre
Department of Mechanics
KTH–Royal Institute of Technology
SE–100 44 Stockholm, Sweden
sohrab@mech.kth.se

ABSTRACT

Over the last decade wind tunnel experiments and numerical simulations have shown that steady spanwise mean velocity gradients are able to attenuate the growth of different types of boundary layer disturbances if introduced in a controlled way. In this paper some different techniques to setup the spanwise mean velocity variations are discussed and their stabilizing effect leading to transition delay are quantified. This control strategy has potential to lead to an unforeseen positive impact on the broad spectrum of industrial applications where reducing drag is a daily challenge.

1 INTRODUCTION

Recent wind tunnel experiments have shown that steady streamwise elongated streaks, produced by the lift-up mechanism, are able to reduce skin-friction drag by delaying transition to turbulence in flat plate boundary layers Fransson *et al.* (2006); Shahinfar *et al.* (2012). Steady streaks may be generated by using either *active* or *passive* boundary-layer modulators, being related to whether external energy is being added or not to the control system in order to perform the control.

The underlying physical mechanism for the stabilizing effect has been shown to be associated with the extra turbulence production term, i.e. the co-variance of the streamwise and spanwise fluctuating velocity components acting on the spanwise gradient of the mean streamwise velocity component, which turns out to be of negative sign Cossu & Brandt (2004). In combination with viscous dissipation it can overcome the wall-normal production term and create an overall stabilizing effect. This control method is today known as the method of spanwise mean velocity gradient and is used as a control strategy within the AFRODITE[1] research program. The Achilles' heel of above-described control method is that the streamwise streaks being set up by some boundary layer modulators can break down to turbulence via a secondary instability, if the streak amplitude exceeds a threshold value. This would lead to an earlier onset of transition and failure of the control would be inevitable.

A recurrent criticism of the described control method is the amount of induced drag due to the presence of the streaks and the extra drag associated with the devices themselves. Even though the control has no cost per se in terms of added energy, the devices will increase the drag, which has to be balanced against the gain. In successive studies Fransson & Talamelli (2012); Shahinfar *et al.* (2013), where miniature vortex generators (MVGs) have been used to generate the streaky base flow, the local skin-friction coefficient has been calculated using the momentum-integral equation and the induced drag has been estimated. For the optimal streak amplitude for transition delay (around 21%) the local skin-friction drag is increased by approximately 10% just behind the MVGs compared to the Blasius boundary layer. The local skin-friction excess decays and at around 300 MVG heights downstream of the MVG array, the boundary layer has recovered and the skin-friction coefficient curve collapses onto the Blasius curve. In order to assess the total drag increase due to the MVG array a direct numerical simulation of the flow around a pair of MVGs giving a streak amplitude of approximately 25% has been performed Camarri *et al.* (2013). In the simulation a flat plate length of $Re_x = xU_\infty/\nu = 4.5\times10^5$, expressed in terms of Reynolds number, was considered. Here x and ν denote the distance from the leading edge and the kinematic viscosity, respectively, and U_∞ is the free-stream velocity. Downstream of this position the modulated boundary layer has recovered and the contribution to the overall drag is identical to the Blasius boundary layer. The total drag increase due to the presence of the MVGs amounts to 2.5%, which is considered fairly cheap when compared with the alternative of

[1] Advanced Fluid Research On Drag reduction In Turbulence Experiments, funded by ERC via a Starting Grant.

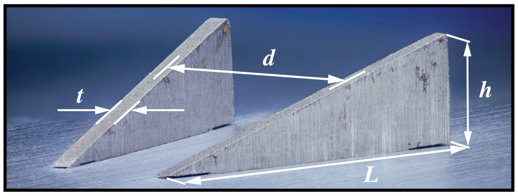

Figure 1. (Photo published in Shahinfar *et al.*, 2012) A photo of a MVG pair with triangular blades. The geometrical parameters: $h = 1.1$, $d = L = 3.25$ and $t = 0.3$ (mm).

a turbulent boundary layer over a laminar one, which can amount to an increase of the local skin-friction coefficient of up to one order of magnitude.

2 EXPERIMENTAL SETUP

Most experiments, within the AFRODITE program, have been performed in the Minimum Turbulence Level (MTL) wind tunnel at the Royal Institute of Technology (KTH) in Stockholm, Sweden. The MTL is a closed circuit tunnel with a test section of 7 m in length and a cross-sectional area of 0.8 m and 1.2 m in height and width, respectively. The flow is provided by an axial fan (DC 85 kW), which can be operated in the range $\simeq 0.5-70$ m s^{-1} in an empty test section. The flow quality in this tunnel is considered to be very good with a background turbulence level of 0.025% of the free stream velocity at 25 m s^{-1} (Lindgren & Johansson, 2002). Downstream of the fan a heat exchanger is installed which is capable of maintaining the circulating air at a constant temperature with a tolerance of ± 0.05 °C above 6 m s^{-1}. The boundary layer experiments were performed on a flat plate positioned horizontally inside the test section. To reduce the leading edge effect by means of reducing the pressure gradient region, an asymmetric leading edge has been used in most experiments (Klingmann *et al.*, 1993) along with an adjustable trailing edge flap. The tunnel coordinates are defined with $(x,\ y,\ z)$ as streamwise, wall-normal and spanwise coordinates. The corresponding velocity components are $(U,\ V,\ W)$, respectively, with small letters denoting velocity perturbations. On top of the roof, of the test section, a five degree traversing mechanism is mounted, which here was used for traversing the measurement probes.

To measure the velocity signal a constant temperature hot-wire anemometer was employed. In all the measurements, a DANTEC Dynamics™ StreamLine 90N10 anemometer system was used and the voltage signals were acquired by a National Instruments™ acquisition board (NI PCI-6259, 16-Bit) with a sampling frequency of 2 kHz. Single wire probes were manufactured *in-house* with Wollaston Platinum wires of 2.54 μm in diameter and 0.7 mm long. The hot-wires were calibrated *in-situ* versus a Prandtl tube connected to a manometer (Furness FC0510). In order to get the best accuracy, especially close to the surface plate where the speed is low, a modified King's law was used as calibration function (Johansson & Alfredsson, 1982).

3 RESULTS

Studies of different types of boundary layer-modulators, both passive and active, have been carried out within the AFRODITE research program. A successful boundary-layer modulator for transition delay has turned out to be the miniature vortex generator Shahinfar *et al.* (2012) (see figure 6) . This passive device is typically placed in an array orthogonal to the direction of the base flow in a flat plate boundary layer, which creates a streaky boundary layer with alternating high and low speed streaks in the spanwise direction. Depending on the configuration with respect to both boundary layer and geometrical parameters of the devices the streaks evolve differently in the streamwise direction. Table 1 summarizes all cases in the latest parameter variation study, where rectangular blades of the MVGs were used. This set of data form the base for the scaling analysis in the next section. This type of analysis is of great importance in the design of new MVGs in completely new flow configurations where skin-friction drag reduction is desired.

3.1 Scaling of the streamwise streaks

The streak amplitude evolution in the streamwise direction is shown in figure 2 for the cases where stable streaks were present in the boundary layer (see table 1). It is observed that the peak amplitude of the streaks is varying with more than 250% with boundary layer and MVG array parameters, i.e. in a range from 19.8% to 53.1% of the free-stream velocity, which is shown by the horizontal grey region. The downstream location of the peak amplitude is varying by 100%, i.e. in the range $x - x_{\rm MVG} =$ 91 to 181 mm, which is shown by the vertical grey region. Considering the initial algebraic growth in the streak amplitudes starting from $x_{\rm MVG}$, which is followed by an exponential decay, Shahinfar *et al.* (2013) proposed a simple function for scaling the streamwise evolution of the streak amplitudes as

$$\mathscr{F} = \{A_{\rm ST}^{\rm int}/A_{\rm ST}^{\rm int*}\} = \xi \cdot e^{-\xi}\,, \qquad (1)$$

with $A_{\rm ST}^{\rm int*}$ being the normalization value for the streak amplitude. In that study triangular bladed MVGs were employed to generate streamwise streaks in the boundary layer, and as reported the proposed function was proven efficient to predict the evolution of all the configurations that generated steady streaks. It was consequently concluded that the viscous decay of the strearmwise streaks, generated by strong streamwise elongated vortices in the presence of MVGs, is of exponential scale, i.e. in contrast with the algebraic decay of the small amplitude three-dimensional instabilities in the boundary layer reported by Luchini (1996). The finding was in agreement with the results reported by Lögdberg *et al.* (2009) where the decay rate of the streamwise vortices in the turbulent boundary layers was shown to be of exponential scale.

The streamwise distribution, also denoted as the streamwise stretching, of the streaks in the boundary layer is corresponding to the variable ξ in Eq. (1). For this variable Shahinfar *et al.* (2013) proposed a general form as

$$\xi = \left[C_{\xi}^{\rm i}\,(x/x_{\rm MVG} - 1)\right]^{C_{\xi}^{\rm ii}}\,, \qquad (2)$$

with $\xi = 1$ corresponding to the downstream location of the

Case	Symbol	h (mm)	Λ (mm)	d (mm)	θ (deg)	β^0	U_∞ (m s^{-1})	h/δ_1^0	Re_h	$A_{\mathrm{ST}}^{\mathrm{int,p}}$ (%)	F
C01	□	1.3	13.00	3.25	6	0.38	6.0	1.02	294	20.7	174.9
C02	★	1.3	13.00	3.25	9	0.38	6.0	1.02	296	30.5	174.1
C03	○	1.3	13.00	3.25	12	0.39	5.9	1.00	283	37.9	183.6
C04	△	1.3	13.00	3.25	15	0.38	5.9	1.01	287	43.4	179.9
C05	▽	1.3	13.00	3.25	18	0.38	6.0	1.01	289	49.5	178.8
C06	◁	1.3	13.00	3.25	9	0.35	6.8	1.10	361	38.2	117.8
C07	▷	1.3	13.00	3.25	9	0.35	6.9	1.11	366	38.6	182.8
C08	◇	1.3	13.00	3.25	9	0.43	5.0	0.90	210	21.7	216.4
C09	■	1.3	13.00	3.25	9	0.35	7.0	1.12	373	38.7	138.0
C10	●	1.3	13.00	3.25	9	0.33	7.7	1.18	433	46.5	123.9
C11	▲	1.3	13.00	3.25	9	0.31	8.5	1.25	493	53.1	113.8
C12	▼	1.3	17.88	3.25	9	0.28	6.0	1.01	290	19.8	177.9
C13	◀	1.3	16.25	3.25	9	0.30	6.0	1.02	295	24.5	174.3
C14	▶	1.3	14.63	3.25	9	0.34	6.0	1.01	291	24.5	177.0
C15	◆	1.3	11.38	3.25	9	0.43	6.0	1.02	295	38.2	174.1
C16	⊕	1.3	9.75	3.25	9	0.51	6.0	1.01	290	39.3	177.9
C17	⊗	1.3	8.13	3.25	9	0.61	6.0	1.01	290	46.1	178.1

Table 1. MVG configurations C01-C17 and resulting boundary layer parameters and streak amplitudes. h denotes the MVG height, Λ the spanwise wavelength, d the distance between two blades in each MVG pair, θ the angle of attack of the blades toward upcoming flow, β^0 the dimensionless spanwise wave number at x_{MVG}, and δ_1^0 the displacement thickness at x_{MVG}. U_∞ and $A_{\mathrm{ST}}^{\mathrm{int,p}}$ are the free-stream velocity and the peak streak amplitude defined in the running text. F is the dimensionless frequency of the forced TS wave.

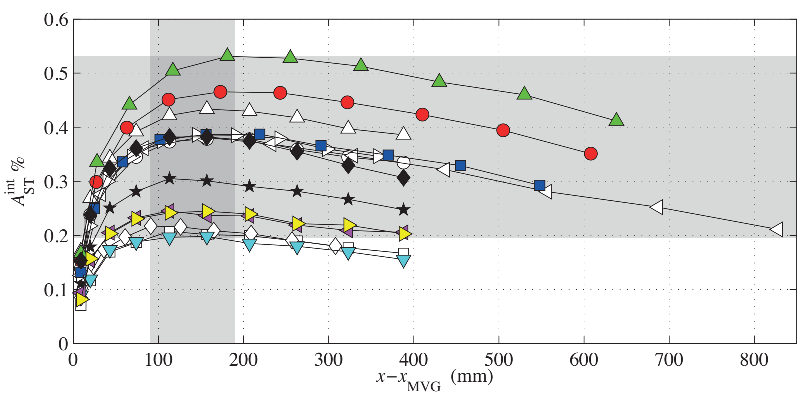

Figure 2. (Figure published in Sattarzadeh & Fransson, 2015). The streak amplitude evolution in the streamwise direction for all the cases with stable streaks. The variation in the maximum streak amplitude as well as the downstream location at which it occurs is depicted by the dark grey area for all the cases. See table 1 for symbols.

peak streak amplitude. Accordingly $A_{\mathrm{ST}}^{\mathrm{int}*}$ in Eq. (1) was set in order to obtain the normalized streak amplitude of $\exp\{-1\} \approx 0.37$ at $\xi = 1$. The scaling relation is tested for the streamwise amplitude evolution of the streaks generated by rectangular bladed MVGs in the present study. The coefficients C_ξ^{i} and C_ξ^{ii} in Eq. (2) together with $A_{\mathrm{ST}}^{\mathrm{int}*}$ in Eq. (1) are determined through fitting the data to the scaling function in Eq. (1) by a least square method for each of the individual cases shown in figure 2. The coefficients are then used to individually scale the streak amplitude evolutions and the result is shown in figure 3. It can be observed that, similar to the streaky boundary layer generated by triangular MVGs, all the cases with stable streaks follow the proposed function in Eq. (1) when rectangular MVGs are employed, although having an even higher modulation in the boundary layer.

The sreamwise stretching of the streaks as well as the peak amplitudes are related to the boundary layer and MVG parameters. Therefore, in order to find a general scaling for all the cases the relation between these parameters and the coefficients C_ξ^{i}, C_ξ^{ii} and $A_{\mathrm{ST}}^{\mathrm{int}*}$ should be determined. For the streamwise stretching of the streaks, as suggested by

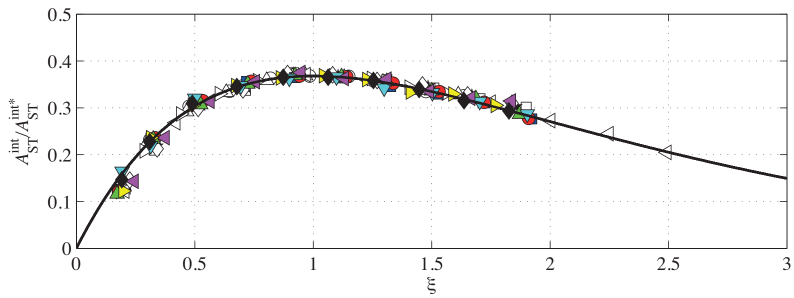

Figure 3. (Figure published in Sattarzadeh & Fransson, 2015). The streak amplitude evolutions for all the cases with stable streaks fitted individually to Eq. (1). The solid line is corresponding to Eq. (1).

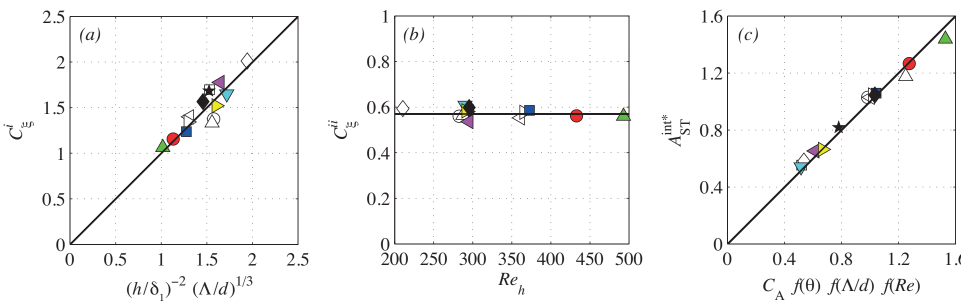

Figure 4. (Figure published in Sattarzadeh & Fransson, 2015). The coefficients $C_\xi^{\rm i}$, $C_\xi^{\rm ii}$ and $A_{\rm ST}^{\rm int*}$, as defined by Eqs. 1 − 4, in (a), (b) and (c), respectively, versus the proposed scaling. The coefficients are determined by means of least square fit of the data to Eq. 1. $f(\theta)$, $f(\Lambda/d)$ and $f(Re)$ in (c) are described in the running text.

α	β	$C_\xi^{\rm ii}$	$C_{\rm A}$	**a**	**b**	**c**	**d**
-2	$1/3$	0.57	1.48×10^{-5}	-2	1.8	4.75	20

Table 2. Coefficients appearing in the proposed scaling of streamwise streaks and determined by means of least square fit to data.

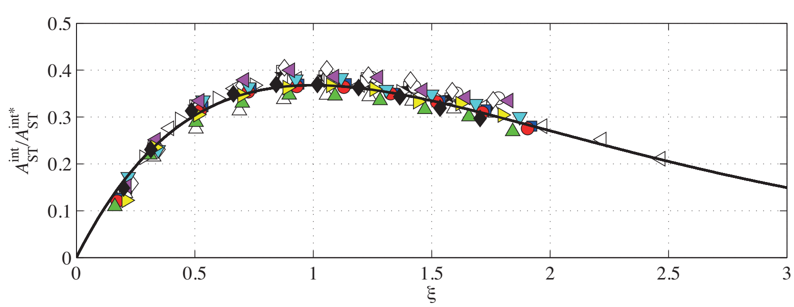

Figure 5. (Figure published in Sattarzadeh & Fransson, 2015). The streak amplitude evolution scaled as proposed in Eqs. (1), (2) and (4) for all cases with stable streaks. The solid line is corresponding to Eq. (1).

Shahinfar *et al.* (2013), $C_\xi^{\rm i}$ can be identified by the ratios $(h/\delta_{\rm I})$ and (Λ/d) as

$$C_\xi^{\rm i} = \left(\frac{h}{\delta_{\rm I}}\right)^{\alpha}\left(\frac{\Lambda}{d}\right)^{\beta}, \quad (3)$$

and $C_\xi^{\rm ii}$ can be found as a constant which is determined together with α and β through a least square fitting method over the data for all cases.

In order to characterize the effect of the spanwise distribution of vortices on $A_{\rm ST}^{\rm int*}$ a new relation as a function of Λ/d was proposed in Sattarzadeh & Fransson (2015). The final scaling of the streak amplitude resulted in

$$A_{\rm ST}^{\rm int*} = C_{\rm A} f(\theta) f(\Lambda/d) f(Re), \quad (4)$$

with the functions of different parameters being

$$f(\theta) = \sin(\theta)\,, \quad (5)$$

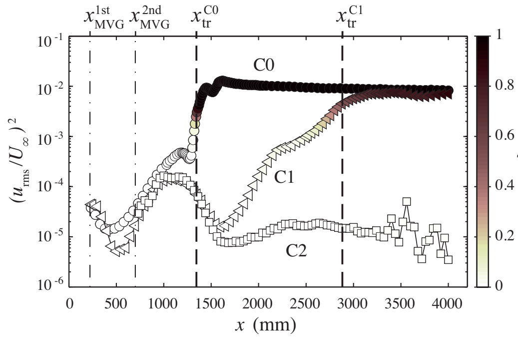

Figure 6. (Figure published in Sattarzadeh *et al.*, 2014). Boundary-layer disturbance energy evolution in the streamwise direction for the cases C0–C2. C0: reference configuration without control. C1: control configuration with one MVG array located at $x^{1st}_{MVG} = 222$ mm. C2: control configuration with two MVG arrays located at x^{1st}_{MVG} and $x^{2nd}_{MVG} = 700$ mm. The color bar applied to the symbols correspond to the intermittency (γ) of the velocity signal. The figure is published in Sattarzadeh *et al.* (2014).

$$f(\Lambda/d) = \left[1 + \frac{e^{\mathbf{a}(\Lambda/d\,-\,\mathbf{c})} - e^{\mathbf{b}(\Lambda/d\,-\,\mathbf{c})}}{\mathbf{d}}\right], \qquad (6)$$

$$f(Re) = \left(\frac{U_\infty h}{\nu}\right)^2. \qquad (7)$$

Here **a**, **b**, **c**, **d** and C_A are determined by means of least square fit to the data. Eq. (5) originates from θ being correlated with the circulation of generated vortices which is proportional to the lift force on the elements, and $f(\theta)$ is therefore characterized by $\sin\theta$. Due to a more systematic variation of Λ/d a new function of $f(\Lambda/d)$ was also proposed which differs from the one proposed in Shahinfar *et al.* (2013). An increase in U_∞ and h both give rise to an increased maximum streak amplitude which scales with $Re^2 = (hU_\infty/\nu)$, which was proposed already in Shahinfar *et al.* (2013). The data for coefficients C^{i}_{ξ} (Eq. 3) and C^{ii}_{ξ}, and the normalization amplitude A^{int*}_{ST} (Eq. 4) are shown in figure 4.

The determined coefficients for Eqs. (2), (3) and (4) are summarized in table 2. The proposed scaling is tested for all the cases with stable streaks and the result is shown in figure 5. The suggested evolution of the streaks with the initial algebraic growth followed by an exponential decay, as proposed in Eq. (1), is shown by the solid black line in the figure. By comparing this figure with figure 2, where the unscaled streak amplitude evolution is depicted, it can be concluded that the suggested scaling relation is efficient to predict the streak amplitude distribution for all cases where stable streaks are generated.

The data shown here are found in Sattarzadeh & Fransson (2015) where also, a detailed report on the stabilizing effect of TS waves is given.

3.2 Net skin-friction drag reduction $>$65%

Unfortunately, the natural recovery of the modulated laminar base flow in the streamwise direction is of exponential space scale and hence the passive laminar control fades away fairly rapidly. In a recent study we have shown that by placing a second array of MVGs downstream of the first one it is possible to nourish the counter-rotating streamwise vortices responsible for the modulation, which results in a prolonged streamwise extent of the control (see figure 6). With this control strategy it is possible to delay the transition to turbulence, consecutively, by reinforcing the control effect and with the ultimate implication of obtaining a net skin-friction drag reduction of at least 65% Sattarzadeh *et al.* (2014).

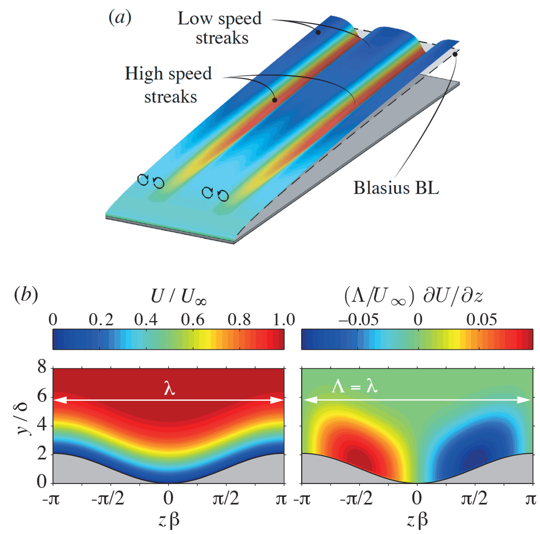

Figure 7. Different techniques to set up spanwise mean velocity gradients as a passive flow control strategy leading to transition delay. (*a*) A sketch of free-stream vortices modulating the boundary layer in the spanwise direction. The sketch is published in Siconolfi et al. Siconolfi *et al.* (2015). (*b*) Wavy surface in the spanwise direction in order to accomplish spanwise mean velocity gradients.

4 New ideas for steady streamwise streaks

Further wind tunnel experiments in the Minimum-Turbulence-Level wind tunnel at KTH are being performed with new passive and active control method approaches. A new passive control approach is directed towards direct surface modulations, in line with the work described in Downs & Fransson (2014), a necessary step in being able to delay transition to turbulence originating from free-stream turbulence according to our current knowledge. A sketch of a wavy surface is shown in figure 7(*b*). Another, control approach reported in Siconolfi *et al.* (2015) is to generate free-stream vortices, which penetrate through the boundary layer edge and modulate the boundary layer from the top (see the sketch in figure 7*a*). This work is numerical so far, but existing ideas on how to setup free-stream vortices experimentally will be tested in the near future.

The conference presentation will include the latest results performed within the AFRODITE program, with focus on the presently ongoing measurements.

JHMF acknowledges the European Research Council for their financial support of the AFRODITE project through a Starting Independent Researcher Grant.

REFERENCES

Camarri, S., Fransson, J. H. M. & Talamelli, A. 2013 Numerical investigation of the afrodite transition control strategy. In *Progress in Turbulence V* (ed. A. Talamelli, M. Oberlack & J. Peinke), pp. 65–69. Springer.

Cossu, C. & Brandt, L. 2004 On Tollmien-Schlichting-like waves in streaky boundary layers. *Eur. J. Mech./B Fluids* **23**, 815–833.

Downs, R. S. & Fransson, J. H. M. 2014 Tollmien-Schlichting wave growth over spanwise-periodic surface patterns. *J. Fluid Mech.* **754**, 39–74.

Fransson, J. H. M. & Talamelli, A. 2012 On the generation of steady streamwise streaks in flat-plate boundary layers. *J. Fluid Mech.* **698**, 211–234.

Fransson, J. H. M., Talamelli, A., Brandt, L. & Cossu, C. 2006 Delaying transition to turbulence by a passive mechanism. *Phys. Rev. Lett.* **96**, 064501.

Johansson, A. V. & Alfredsson, P. H. 1982 On the structure of turbulent channel flow. *J. Fluid Mech.* **122**, 295–314.

Klingmann, B. G. B., Boiko, A., Westin, K. J. A., Kozlov, V. V. & Alfredsson, P. H. 1993 Experiments on the stability of Tollmien-Schlichting waves. *Eur. J. Mech. B/Fluids* **12**, 493–514.

Lindgren, B. & Johansson, A. V. 2002 Evaluation of the flow quality in the mtl wind-tunnel. *Tech. Rep. KTH/MEK/TR–02/13–SE, KTH Mechanics, Stockholm* .

Lögdberg, O., Fransson, J. H. M. & Alfredsson, P. H. 2009 Streamwise evolution of longitudinal vortices in a turbulent boundary layer. *J. Fluid Mech.* **623**, 27–58.

Luchini, P. 1996 Reynolds-number independent instability of the boundary layer over a flat surface. *J. Fluid Mech.* **327**, 101–115.

Sattarzadeh, S. S. & Fransson, J. H. M. 2015 On the scaling of streamwise streaks and their efficiency to attenuate tollmien-schlichting waves. *Exp. Fluids* **56:58**, 58.

Sattarzadeh, S. S., Fransson, J. H. M., Talamelli, A. & Fallenius, B. E. G. 2014 Consecutive turbulence transition delay with reinforced passive control. *Phys. Rev. E* **89**, 061001(R).

Shahinfar, S., Fransson, J. H. M., Sattarzadeh, S. S. & Talamelli, A. 2013 Scaling of streamwise boundary layer streaks and their ability to reduce skin-friction drag. *J. Fluid Mech.* **733**, 1–32.

Shahinfar, S., Sattarzadeh, S. S., Fransson, J. H. M. & Talamelli, A. 2012 Revival of classical vortex generators now for transition delay. *Phys. Rev. Lett.* **109**, 074501.

Siconolfi, L., Camarri, S. & Fransson, J. H. M. 2015 Boundary layer stabilization using free-stream vortices. *J. Fluid Mech.* **764**, R2.